

A Unified Energy-Reservoir Model Containing Contributions from ^{56}Ni and Neutron Stars and Its Implication to Luminous Type Ic Supernovae

S. Q. Wang^{1,2}, L. J. Wang^{1,2}, Z. G. Dai^{1,2} and X. F. Wu^{3,4,5}

¹*School of Astronomy and Space Science, Nanjing University, Nanjing 210093, China; dzg@nju.edu.cn*

²*Key Laboratory of Modern Astronomy and Astrophysics (Nanjing University), Ministry of Education, China*

³*Purple Mountain Observatory, Chinese Academy of Sciences, Nanjing, 210008, China*

⁴*Chinese Center for Antarctic Astronomy, Chinese Academy of Sciences, Nanjing, 210008, China*

⁵*Joint Center for Particle Nuclear Physics and Cosmology of Purple Mountain Observatory-Nanjing University, Chinese Academy of Sciences, Nanjing 210008, China*

ABSTRACT

Most type-Ic core-collapse supernovae (CCSNe) produce ^{56}Ni and neutron stars (NSs) or black holes (BHs). The dipole radiation of nascent NSs has usually been neglected in explaining supernovae (SNe) with peak absolute magnitude M_{peak} in any band are $\gtrsim -19.5$ mag, while the ^{56}Ni can be neglected in fitting most type-Ic superluminous supernovae (SLSNe Ic) whose M_{peak} in any band are $\lesssim -21$ mag, since the luminosity from a magnetar (highly magnetized NS) can outshine that from a moderate amount of ^{56}Ni . For luminous SNe Ic with $-21 \lesssim M_{\text{peak}} \lesssim -19.5$ mag, however, both contributions from ^{56}Ni and NSs cannot be neglected without serious modeling, since they are not SLSNe and the ^{56}Ni mass could be up to $\sim 0.5M_{\odot}$. In this paper we propose a unified model that contain contributions from both ^{56}Ni and a nascent NS. We select three luminous SNe Ic-BL, SN 2010ay, SN 2006nx, and SN 14475, and show that, if these SNe are powered by ^{56}Ni , the ratio of M_{Ni} to M_{ej} are unrealistic. Alternatively, we invoke the magnetar model and the hybrid ($^{56}\text{Ni} + \text{NS}$) model and find that they can fit the observations, indicating that our models are valid and necessary for luminous SNe Ic. Owing to the lack of late-time photometric data, we cannot break the parameter degeneracy and thus distinguish among the model parameters, but we can expect that future multi-epoch observations of luminous SNe can provide stringent constraints on ^{56}Ni yields and the parameters of putative magnetars.

Subject headings: stars: magnetars, - supernovae: general, - supernovae: individual (SN 2010ay, SN 2006nx, SN 14475)

1. Introduction

It has long been believed that most aged massive (zero-age main-sequence mass $M_{\text{ZAMS}} \gtrsim 8.0M_{\odot}$) stars terminate their lives as core-collapse supernovae (CCSNe) (Woosley et al. 2002; Janka et al. 2007), which are classified into type IIP, IIL, IIn, IIb, Ib and Ic according to their spectra and light curves (Filippenko 1997), leaving neutron stars (NSs) or black holes (BHs) at the center and producing a moderate amount of ^{56}Ni which is generally regarded as the dominant power source for most supernovae (SNe) (Colgate & McKee 1969; Colgate et al. 1980; Arnett 1982)¹. Of all these subclasses, SNe Ic have attracted more and more attentions since a great number of these events have been discovered and confirmed in recent years that some SNe Ic with broad absorption line features (“broad-lined” or “BL”) have an accompanying gamma-ray burst (GRB) or X-ray flash (XRF) (Woosley & Bloom 2006; Hjorth & Bloom 2012). Main models of central engines of GRBs associated with SNe are the “collapsar” model (Woosley 1993; MacFadyen & Woosley 1999) involving “BH + disk” systems and the magnetar (highly magnetized neutron star) model (Usov 1992; Metzger et al. 2007; Bucciantini et al. 2008; Metzger et al. 2011) proposing that the explosions may leave behind fast-rotating magnetars, being also regarded as the origin of the shallow decays and plateaus as well as rebrightenings in the multi-band afterglows of some GRBs (Dai & Lu 1998a,b; Zhang & Mészáros 2001; Dai 2004; Dai & Liu 2012).

On the other hand, in the last two decades, optical–NIR and radio observations have revealed that not every SN Ic-BL associates with a GRB or an XRF (Soderberg et al. 2005; Drout et al. 2011). Many SNe Ic-BL, no matter whether they are associated a(n) GRB/XRF or not, have very high kinetic energy $E_K \gtrsim 1.0 \times 10^{52}$ erg and have therefore been called “Hypernovae” (Iwamoto et al. 1998). Supposing that the optical–NIR emission is powered by radioactive ^{56}Ni decay, these SNe Ic need $\sim 0.1 - 0.5M_{\odot}$ of ^{56}Ni . All GRBs associated SNe Ic and most GRB-less SNe Ic are not very luminous, with peak absolute magnitude $M_{\text{peak}} \gtrsim -19.5$.

¹Since the observations for SN 1987A (Lundqvist et al. 2001) and SN 1998bw (Sollerman et al. 2002) have already revealed that the radioactive elements other than ^{56}Ni (e.g., ^{57}Ni , ^{44}Ti and ^{22}Na , etc) constitute only a minor fraction of the radioactive masses and contribute dominant fluxes at very late times ($\gtrsim 600$ days and 1,200–1,400 day after explosion for SN 1987A and SN 1998bw, respectively), we only consider the contribution of ^{56}Ni , which is the most abundant nucleus resulting from explosive silicon burning in shock-heated silicon shells and the dominant energy source at early-time (e.g., ≤ 500 days) of a SN.

Thanks to the unprecedented boom of targeted- and untargeted- sky survey programs, many superluminous SNe (SLSNe) whose M_{peak} in any band are $\lesssim -21$ mag (Gal-Yam 2012) have been found in the past decade, most of which cannot be explained by the widely adopted ^{56}Ni decay model (Quimby et al. 2011; Inserra et al. 2013; Nicholl et al. 2013; McCrum et al. 2014; Nicholl et al. 2014), motivating researchers to consider alternative energy-reservoir models. Currently, main models explaining the SLSNe are SN ejecta - circumstellar medium (CSM) interaction model (Chevalier 1982; Chevalier & Fransson 1994; Chevalier & Irwin 2011; Ginzburg & Balberg 2012) that has been employed to explain many Type IIn luminous SNe (Chugai 1994; Zhang et al. 2012; Ofek et al. 2013) and superluminous SNe IIn (Smith & McCray 2007; Moriya et al. 2013) as well as some Type Ic SLSNe (Chatzopoulos et al. 2013; Nicholl et al. 2014), and the magnetar-powered SLSNe model (Kasen & Bildsten 2010; Woosley 2010) that has been used to explain many Type Ic SLSNe (Inserra et al. 2013; Nicholl et al. 2013; Howell et al. 2013; McCrum et al. 2014; Vreeswijk et al. 2014; Nicholl et al. 2014; Wang et al. 2015). In some cases, the magnetar-powered SLSNe model with the assumption of full energy trapping fails to fit the late-time light curves (Inserra et al. 2013; Nicholl et al. 2014). In Wang et al. (2015), we generalized the magnetar-powered SLSNe model by introducing the hard emission leakage and solved this problem, highlighting the importance of the leakage effect in this model.

Thus, the power sources of most normal SNe and SLSNe have been attributed to ^{56}Ni -decay and the magnetar spin-down or ejecta-CSM interaction, respectively. Within this picture, the dipole radiation of nascent magnetars has usually been neglected in explaining the SNe with $M_{\text{peak}} \gtrsim -19.5$ (but see Maeda et al. 2007), while the ^{56}Ni decay energy have generally been ignored in fitting all Type Ic SLSNe ($M_{\text{peak}} \lesssim -21$) because the peak-luminosity due to the energy injection from a newly born fast-rotating (initial period \sim millisecond) magnetar can outshine that from a moderate amount of ^{56}Ni (see Inserra et al. 2013, for further analysis).

Besides normal SNe and SLSNe mentioned above, however, there are some SNe with $-21 \lesssim M_{\text{peak}} \lesssim -19.5$ mag, constituting a class of “gap-filler” events that bridge normal SNe and SLSNe, have been found by many telescopes. Most of these “gap-filler” SNe are explained by the ^{56}Ni decay model for SNe Ic as well as “Super-Chandrasekhar-Mass” SNe Ia, and the ejecta-CSM interaction model for SNe IIn.

Among these “gap-filler” SNe with $-21 \lesssim M_{\text{peak}} \lesssim -19.5$ mag, luminous Type Ic SNe and their energy-reservoir mechanisms have not attracted enough attentions yet, their high peak-luminosities are simply attributed to the ^{56}Ni cascade decay without any detailed modeling. It has recently been demonstrated that the ^{56}Ni -decay model cannot be arbitrarily used to explain all SNe Ic especially those very luminous ones (Inserra et al. 2013;

Nicholl et al. 2013) since the production of ^{56}Ni is ineffective in CCSNe and more ^{56}Ni mass needs more mass of the ejecta, which could theoretically result in broad light curves that usually conflict with observations. While the CSM-interaction model can predict a wide range of peak luminosities and therefore explain the normal, luminous, and superluminous SNe IIn as a whole category, ^{56}Ni -decay model cannot explain luminous SNe Ic.

Here, we propose that for some luminous SNe Ic, there are other energy reservoirs that play a significant role in producing light curves. Since all hydrogen envelopes of progenitors of SNe Ic have been stripped and the spectra are lack of narrow and/or emission lines indicative of the interactions², we can exclude the ionized hydrogen re-combination (Falk & Arnett 1977; Klein & Chevalier 1978; Popov 1993; Kasen & Woosley 2009) and do not consider the ejecta-CSM interaction process. Therefore, like the cases of SLSNe Ic, the nascent magnetar embedded in the center of the explosion is the most promising candidate for the additional power source (Ostriker & Gunn 1971). On the other hand, the production of ^{56}Ni is inevitable and cannot be neglected in modeling luminous SNe Ic because their peak luminosities are considerably lower than that of SLSNe and the contributions from a moderate amount of ^{56}Ni can be comparable with the contributions given by any other energy reservoirs. Furthermore, in principle, the contributions from ^{56}Ni and NSs cannot be directly neglected for CCSNe with a wide range of peak luminosities. Thus, it is necessary to consider a unified model containing contributions from both ^{56}Ni and NSs.

In this paper we construct the unified model which contain the contributions from both the ^{56}Ni cascade decay energy and the NS rotational energy, and apply it to explain the light curves of some luminous SNe Ic-BL, i.e., SN 2010ay, SN 2006nx, and SN 14475. The remainder of this paper is organized as follows. In Section 2, we give a unified semi-analytical model for Type Ic SNe. Based on this model, we fit the light curves of SN 2010ay, SN 2006nx, and SN 14475 in Section 3. Finally, some discussions and conclusions are presented in Section 4.

2. The unified semi-analytical model for SNe

In this section, we construct a unified semi-analytical model combining energy from a spin-down magnetar and an amount of ^{56}Ni to describe the SN luminosity evolution. In this unified model, ^{56}Ni release high energy photons via the cascade decay chain $^{56}\text{Ni} \rightarrow ^{56}\text{Co} \rightarrow ^{56}\text{Fe}$, while the magnetar can inject its rotational energy into the SN ejecta as heat energy

²the unique exception is SN 2010mb which cannot be explained by ^{56}Ni -powered model and has a signature of interactions (Ben-Ami et al. 2014)

(Ostriker & Gunn 1971).

Based on Arnett (1982), taking into account the γ -ray and X-ray leakage (e.g., Clocchiatti & Wheeler 1997; Valenti et al. 2008; Chatzopoulos et al. 2009, 2012; Drout et al. 2013; Wang et al. 2015), the luminosity is given by

$$L(t) = \frac{2}{\tau_m} e^{-\left(\frac{t^2}{\tau_m^2} + \frac{2R_0 t}{v\tau_m^2}\right)} (1 - e^{-\tau_\gamma(t)}) \int_0^t e^{\left(\frac{t'^2}{\tau_m^2} + \frac{2R_0 t'}{v\tau_m^2}\right)} \times \left(\frac{R_0}{v\tau_m} + \frac{t'}{\tau_m}\right) P(t') dt' \text{ erg s}^{-1}, \quad (1)$$

where R_0 is the initial radius of the progenitor, which is very small compared to the radius of the ejecta. We take the limit $R_0 \rightarrow 0$, then the above equation can be largely simplified. With Equations (18), (19) and (22) of Arnett (1982), the effective light-curve timescale τ_m can be written as ³

$$\tau_m = \left(\frac{2\kappa M_{\text{ej}}}{\beta v c}\right)^{1/2}, \quad (2)$$

where κ is the optical opacity to optical photons (i.e., the Thomson electron scattering opacity), M_{ej} and v are the mass and expansion speed of the ejecta, respectively, and c is the speed of light. $\beta \simeq 13.8$ is a constant that accounts for the density distribution of the ejecta. $P(t)$ is the power function. Here, v is the scale velocity (v_{sc}) in Arnett (1982) and approximates to the photospheric expansion velocity v_{ph} . Hereafter, we let $v \simeq v_{\text{ph}}$.

The factors $e^{-\tau_\gamma(t)}$ and $(1 - e^{-\tau_\gamma(t)})$ in Equation (1) represent the γ -ray leakage and trapping rate, respectively. $\tau_\gamma(t) = At^{-2}$ is the optical depth to γ -rays (Chatzopoulos et al. 2009, 2012). If the SN ejecta has a uniform density distribution ($M_{\text{ej}} = (4/3)\pi\rho R^3$, $E_K = (3/10)M_{\text{ej}}v^2$), A depends on κ_γ (the opacity to γ -rays), M_{ej} and v as

$$\begin{aligned} A &= \frac{3\kappa_\gamma M_{\text{ej}}}{4\pi v^2} \\ &= 4.75 \times 10^{13} \left(\frac{\kappa_\gamma}{0.1 \text{ cm}^2 \text{ g}^{-1}}\right) \\ &\quad \times \left(\frac{M_{\text{ej}}}{M_\odot}\right) \left(\frac{v}{10^9 \text{ cm s}^{-1}}\right)^{-2} \text{ s}^2, \end{aligned} \quad (3)$$

³The coefficient 2 in the equation has been adopted as $\frac{10}{3}$ in some other papers (Chatzopoulos et al. 2009, 2012, 2013; Wang et al. 2015), the latter originated from a typo in Equation (54) of Arnett (1982) that written 5/3 as 3/5, see also the footnote 1 in Wheeler et al. (2014). To get the same light curves, κ or M_{ej} (v) should be multiplied by 5/3 (3/5), or these three parameters simultaneously adjusted so that τ_m can be invariant for an individual event.

2.1. The ^{56}Ni -decay energy model

In the ^{56}Ni -decay energy model, the input power is

$$P(t) = P_{\text{Ni}}(t) = \epsilon_{\text{Ni}} M_{\text{Ni}} e^{-t/\tau_{\text{Ni}}} + \epsilon_{\text{Co}} M_{\text{Ni}} \frac{e^{-t/\tau_{\text{Co}}} - e^{-t/\tau_{\text{Ni}}}}{1 - \tau_{\text{Ni}}/\tau_{\text{Co}}} \text{ erg s}^{-1}, \quad (4)$$

where $\epsilon_{\text{Ni}} = 3.9 \times 10^{10} \text{ erg s}^{-1} \text{ g}^{-1}$ is the energy generation rate per unit mass due to ^{56}Ni decay ($^{56}\text{Ni} \rightarrow ^{56}\text{Co}$) (Cappellaro et al. 1997; Sutherland & Wheeler 1984), M_{Ni} is the initial mass of ^{56}Ni , $\tau_{\text{Ni}} = 8.8$ days is the e -folding time of the ^{56}Ni decay, $\epsilon_{\text{Co}} = 6.8 \times 10^9 \text{ erg s}^{-1} \text{ g}^{-1}$ is the energy generation rate due to ^{56}Co decay ($^{56}\text{Co} \rightarrow ^{56}\text{Fe}$) (Maeda et al. 2003), $\tau_{\text{Co}} = 111.3$ days is the e -folding time of the ^{56}Co decay.

2.2. The magnetar spin-down energy model

In the magnetar model, supposing that all the spin-down energy released can be converted into the heat energy of SN ejecta and the angle between the dipole magnetic fields and the magnetar's spin axis is 45° , the power coming from the magnetar dipole radiation is (Ostriker & Gunn 1971)

$$P(t) = P_{\text{NS}}(t) = \frac{E_{\text{NS}}}{\tau_{\text{NS}}} \frac{1}{(1 + t/\tau_{\text{NS}})^2} \text{ erg s}^{-1}, \quad (5)$$

$\tau_{\text{NS}} = 6 I_{\text{NS}} c^3 / B^2 R_{\text{NS}}^6 \Omega_0^2 = 1.3 (B/10^{14} \text{ G})^{-2} (P_0/10 \text{ ms})^2 \text{ yr}$ is the spin-down timescale of the magnetar (Kasen & Bildsten 2010). E_{NS} is the rotational energy of the magnetar,

$$\begin{aligned} E_{\text{NS}} &\simeq (1/2) I_{\text{NS}} \Omega_{\text{NS}}^2 \\ &\simeq 2 \times 10^{52} \frac{M_{\text{NS}}}{1.4 M_\odot} \left(\frac{P_0}{1 \text{ ms}} \right)^{-2} \left(\frac{R_{\text{NS}}}{10 \text{ km}} \right)^2 \text{ erg}, \end{aligned} \quad (6)$$

where M_{NS} , R_{NS} and P_0 are the mass, radius and initial rotational period of the magnetar, respectively, while $I_{\text{NS}} = (2/5) M_{\text{NS}} R_{\text{NS}}^2$ is the moment of inertia of the magnetar whose canonical value is $\sim 10^{45} \text{ g cm}^2$ (Woosley 2010).

2.3. The hybrid (^{56}Ni + magnetar) model

If an amount of ^{56}Ni is synthesized and a fast-rotating magnetar is left after a SN explosion, both contributions from these two power sources must be taken into account, this is the hybrid model. In this model, the luminosity of a SN is

$$L_{\text{uni}}(t) = L_{\text{Ni}}(t) + L_{\text{NS}}(t), \quad (7)$$

where $L_{\text{Ni}}(t)$ and $L_{\text{NS}}(t)$ are luminosities supplied by ^{56}Ni and the magnetar, respectively.

In this paper we propose the “unified” model that contains the above three models, i.e., the ^{56}Ni model, the magnetar model, and the hybrid model. If the contribution from the magnetar or ^{56}Ni can be neglected, this model would be simplified to the magnetar model or the ^{56}Ni -decay model, respectively. The parameter set for the unified model is $(M_{\text{ej}}, v, M_{\text{Ni}}, B, P_0, \kappa_\gamma)$. When $M_{\text{Ni}} = 0$, the parameter set is $(M_{\text{ej}}, v, B, P_0, \kappa_\gamma)$, corresponding to the magnetar model; when the neutron star is non-rotational, the parameter set is $(M_{\text{ej}}, v, M_{\text{Ni}}, \kappa_\gamma)$, corresponding to the ^{56}Ni -decay model; when the contributions from ^{56}Ni and the magnetar are both important, the model can be termed as the hybrid model. It should be noted that if the photospheric velocity v_{ph} is not measured, then $v \simeq v_{\text{ph}}$ is also a free parameter.

3. Fits to the light curves of SN 2010ay, SN 2006nx, and SN 14475

To verify this unified model, we select three luminous SNe Ic-BL, SN 2010ay, SN 2006nx, and SN 14475. SN 2010ay was discovered by the Catalina Real-time Transient Survey (CRTS; Drake et al. 2009) with V-Band and R-Band peak absolute magnitudes, $M_V \approx -19.4$ mag and $M_R \approx -20.2 \pm 0.2$ mag, respectively. We use the R-band light curve as a proxy for the bolometric light curve of SN 2010ay. Although the former is not a completely reliable proxy for the latter in some cases (e.g., Walker et al. 2014), Wheeler et al. (2014) pointed out that, for SN 1993J (Type IIb), SN 1998bw (Ic-BL) and SN 2002ap (Ic-BL), the discrepancies between the R-band light curves and the quasi-bolometric light curves are rather small and can be neglected.

SN 2006nx and SN 14475 were discovered by the SDSS-II (Taddia et al. 2015) with peak absolute bolometric magnitude ≈ -20.36 mag and ≈ -20.1 mag, respectively. Taddia et al. (2015) have constructed their bolometric light curves, so hereafter we adopt their data.

The peak luminosities of SN 2010ay, SN 2006nx, and SN 14475 are ~ 4.2 , 4.84 , and 3.8 times that of SN 1998bw which is a well-studied SN Ic-BL with peak absolute magnitude ~ -18.65 and the ^{56}Ni mass $\sim 0.43_{-0.05}^{+0.05} M_\odot$ (Mazzali et al. 2006), respectively. Hence, SN 2010ay, SN 2006nx, and SN 14475 are luminous SNe/HNe and brighter than all GRB-associated SNe/HNe confirmed to date.

The so-called Arnett law (Arnett 1979, 1982) reports that the peak luminosity of a SN purely powered by ^{56}Ni decay is proportional to the instantaneous energy deposi-

tion, therefore is proportional to the initial ^{56}Ni mass ⁴, which is widely invoked to infer the ^{56}Ni yields of some SNe (Contardo et al. 2000; Strolger et al. 2002; Candia et al. 2003; Stritzinger & Leibundgut 2005; Yuan et al. 2010; Cano et al. 2014). Comparing to the type Ic supernova SN 1998bw, the ^{56}Ni yields of SN 2010ay, SN 2006nx, and SN 14475 are estimated to be $1.81_{-0.21}^{+0.21} M_{\odot}$, $2.08_{-0.24}^{+0.24} M_{\odot}$, and $1.63_{-0.19}^{+0.19} M_{\odot}$, respectively, when the Arnett law is applied. The value $M_{\text{Ni}} \sim 1.81_{-0.21}^{+0.21} M_{\odot}$ for SN 2010ay is considerably larger than the value $0.9_{-0.1}^{+0.1} M_{\odot}$ derived in Sanders et al. (2012) while the above values of M_{Ni} , $2.08_{-0.24}^{+0.24} M_{\odot}$ for SN 2006nx and $1.63_{-0.19}^{+0.19} M_{\odot}$ for SN 14475 are roughly consistent with the values $M_{\text{Ni}} = 1.86_{-0.12}^{+0.12} M_{\odot}$ and $M_{\text{Ni}} = 1.27_{-0.09}^{+0.08} M_{\odot}$ for the two SNe derived in Taddia et al. (2015).

The inferred ejecta masses of SN 2010ay, SN 2006nx, and SN 14475 are $M_{\text{ej}} \approx 4.7 M_{\odot}$ (Sanders et al. 2012), $7.52_{-1.74}^{+4.83} M_{\odot}$ (Taddia et al. 2015), and $2.90_{-1.48}^{+3.38} M_{\odot}$ (Taddia et al. 2015), respectively. Hence, the ratios of M_{Ni} to M_{ej} are ~ 0.4 , ~ 0.2 , and $\sim 0.2 - 0.4$ for SN 2010ay, SN 2006nx, and SN 14475, respectively. These values far exceed the values of all GRB-associated SNe, which are typically $\sim 0.05 - 0.1$ (Sanders et al. 2012) and larger than the upper limit (~ 0.2) for CCSNe (Umeda & Nomoto 2008). The above analysis suggests that there should be other energy sources aiding these three SNe to the high peak luminosities. As mentioned above, power from ionized element re-combination and CSM-interaction can be safely neglected, we focus on the contributions of ^{56}Ni and the magnetar possibly leaved behind the stellar explosion.

In this section, we use equations given in Section 2 to reproduce the semi-analytical light curves and fit the observations of SN 2010ay, SN 2006nx, and SN 14475. We assume that the fiducial value of the optical opacity κ is 0.07 (e.g., Taddia et al. 2015). The photospheric expansion velocity v_{ph} of SN 2010ay, SN 2006nx, and SN 14475 are $\approx 1.92 \times 10^4 \text{ km s}^{-1}$ (0.064 c) (Sanders et al. 2012), $\approx 1.54 \times 10^4 \text{ km s}^{-1}$ (0.051 c), and $\approx 1.87 \times 10^4 \text{ km s}^{-1}$ (0.062 c) (Taddia et al. 2015), respectively. Thus v is no longer a free parameter in our fitting.

In many light-curve modeling, κ_{γ} has been assumed to have a fiducial value $0.027 \text{ cm}^2 \text{ g}^{-1}$

⁴Strictly speaking, the peak luminosity of a SN depends sensitively upon the opacity, initial ^{56}Ni mass, ejecta mass and kinetic energy. Only if the varieties other than ^{56}Ni mass are same for SNe or their effects on changing the peak luminosities of SNe can be canceled each other (e.g., higher opacity and lower ejecta mass, etc), then the peak luminosities of SNe are proportional to the initial ^{56}Ni mass. These conditions could be satisfied in many SNe, so the Arnett law can be used to infer the ^{56}Ni mass of SNe by comparing them to well-studies SNe (e.g., SN 1987A, etc) which have precise measurements of ^{56}Ni masses and bolometric light curves. In Section 3.1, we will use the ^{56}Ni -decay model to reproduce the light curves of SN 2010ay, SN 2006nx and SN 14475, and examine the ^{56}Ni masses derived by the Arnett law.

for the ^{56}Ni -powered SNe Ic (e.g., Cappellaro et al. 1997; Mazzali et al. 2000; Maeda et al. 2003) and $\gtrsim 0.01 \text{ cm}^2 \text{ g}^{-1}$ for the magnetar-powered SNe (see Kotera et al. 2013, Fig. 8), respectively. It is worth emphasizing that in the magnetar model, κ_γ can vary between ~ 0.01 and $0.2 \text{ cm}^2 \text{ g}^{-1}$ ($E_\gamma \gtrsim 10^6 \text{ eV}$) while κ_X can vary between ~ 0.2 and $10^4 \text{ cm}^2 \text{ g}^{-1}$ ($10^2 \text{ eV} \lesssim E_X \lesssim 10^6 \text{ eV}$) (see Kotera et al. 2013, Fig. 8). Therefore, κ_γ is also a free parameter in our fitting.

3.1. The ^{56}Ni -decay energy model

The parameters for the ^{56}Ni -powered model are listed in Table 1 and the light curves reproduced by these sets of parameters are shown in Fig. 1 (Models A1 and A2 for SN 2010ay, B1 and B2 for SN 2006nx, C1 and C2 for SN 14475).

Using the empirical relation between the peak absolute magnitude and the mass of ^{56}Ni derived by Drout et al. (2011), Sanders et al. (2012) inferred that the ^{56}Ni mass of SN 2010ay is $0.9_{-0.1}^{+0.1} M_\odot$. However, it can be seen from Fig. 1 and Table 1 that $1.0 M_\odot$ of ^{56}Ni is inadequate to power the peak luminosity of SN 2010ay solely. To power the peak luminosity, $\sim 2.0 M_\odot$ of ^{56}Ni must be required. The value $2.0 M_\odot$ is consistent with the value $1.81_{-0.21}^{+0.21} M_\odot$ derived by the Arnett law.

It can be seen from Fig. 1 and Table 1 that $2.0 M_\odot$ and $1.3 M_\odot$ of ^{56}Ni are required to power the peak luminosities of SN 2006nx and SN 14475, respectively. The values $2.0 M_\odot$ and $1.3 M_\odot$ are consistent with the value $1.86_{-0.12}^{+0.12} M_\odot$ and $1.27_{-0.09}^{+0.08} M_\odot$ derived by Taddia et al. (2015) as well as the values $2.08_{-0.24}^{+0.24} M_\odot$ and $1.63_{-0.19}^{+0.19} M_\odot$ derived by the Arnett law.

In this paper, we adopt a fiducial value of optical opacity $0.07 \text{ cm}^2 \text{ g}^{-1}$. In many other papers, however, the fiducial values of opacity have also been assumed to be $0.06 \text{ cm}^2 \text{ g}^{-1}$ (e.g., Valenti et al. 2011; Lyman et al. 2014), $0.08 \text{ cm}^2 \text{ g}^{-1}$ (e.g., Arnett 1982; Mazzali et al. 2000), $0.10 \text{ cm}^2 \text{ g}^{-1}$ (e.g., Nugent et al. 2011; Inserra et al. 2013; Wheeler et al. 2014) and $0.2 \text{ cm}^2 \text{ g}^{-1}$ (e.g., Kasen & Bildsten 2010; Nicholl et al. 2014). It is necessary to point out that more ^{56}Ni for the ^{56}Ni model or smaller P_0 of the magnetar for the magnetar model is required to account for the peak luminosity of SN 2010ay, SN 2006nx, and SN 14475 when κ is larger than $0.07 \text{ cm}^2 \text{ g}^{-1}$ since larger κ results in larger diffusion time and lower the peak luminosities. On the other hand, when κ is smaller than $0.07 \text{ cm}^2 \text{ g}^{-1}$, less ^{56}Ni or larger P_0 are required for the same peak luminosity. For example, If we assume that SN 2010ay is powered by ^{56}Ni and $\kappa = 0.06 \text{ cm}^2 \text{ g}^{-1}$, then $\sim 1.8 M_\odot$ of ^{56}Ni must be synthesized, which is smaller than $2.0 M_\odot$ when $\kappa = 0.07 \text{ cm}^2 \text{ g}^{-1}$.

To maintain the same peak luminosities and shapes of light curves, $\kappa M_{\text{ej}}/v$ must be

invariant. Because the photospheric velocities of SN 2010ay, SN 2006nx, and SN 14475 are fixed, so $\kappa M_{\text{ej}} = \text{constant}$ is required. Hence, smaller κ requires larger M_{ej} , as illustrated in Fig. 2.

3.2. The upper limits of ^{56}Ni mass

A consensus has been reached that iron–core-collapse SNe can synthesize a large amount of ^{56}Ni . However, could these 3 SN explosions produce $\sim 1.3 M_{\odot}$ or $\sim 2.0 M_{\odot}$ of ^{56}Ni ? To get reasonable upper limits for the ^{56}Ni masses synthesized in the explosions of SN 2010ay, SN 2006nx, and SN 14475, we perform semi-quantitative estimates.

The radius of the ^{56}Ni layer can be given as

$$\begin{aligned} R_{\text{Ni}} &= \left(\frac{E_{\text{exp}} + E_{\text{bin}}}{\frac{4}{3}\pi a T^4} \right)^{1/3} \\ &\simeq 4.0 \times 10^3 \left(\frac{E_{\text{exp}} + E_{\text{bin}}}{10^{51} \text{ erg}} \right)^{1/3} \left(\frac{T}{5 \times 10^9 \text{ K}} \right)^{-4/3} \text{ km} \end{aligned} \quad (8)$$

where E_{exp} , E_{bin} are the explosion energy and the binding energy of the progenitor, respectively, T is the temperature of the ejecta, $a = 7.56566 \times 10^{15} \text{ erg cm}^{-3} \text{ K}^{-4}$ is the radiation energy density constant. Since $M_{\text{Ni}} = 4/3 \rho_{\text{Ni}} \pi R_{\text{Ni}}^3$, M_{Ni} is therefore approximately proportional to $E_{\text{exp}} + E_{\text{bin}} \simeq E_{\text{exp}}$ ⁵ which in turn is approximately proportional to the kinetic energy E_{K} , see, e.g., the bottom panel of Fig. 7 of Hamuy (2003) and the left panel of Fig. 23 of Pejcha & Thompson (2014). The masses of the progenitors also influence the yields of ^{56}Ni . These facts can also be seen in Fig. 7 and Table 3 in Umeda & Nomoto (2008). The typical masses of the ^{56}Ni synthesized during the explosive silicon burning are $\sim 0.1 - 0.5 M_{\odot}$ for CCSNe.

We compare SN 2010ay, SN 2006nx, and SN 14475 with the prototype hypernova SN 1998bw. The kinetic energy of SN 2010ay ($\approx 1.1 \times 10^{52} \text{ erg}$, Sanders et al. 2012) and SN 14475 ($\approx 4.71_{-2.41}^{+12.29} \times 10^{51} \text{ erg}$, Taddia et al. 2015) are about a factor of 3-5 smaller than that of SN 1998bw ($\approx 3 - 5 \times 10^{52} \text{ erg}$, Iwamoto et al. 1998; Nakamura et al. 2001; Lyman et al. 2014), so we can infer that their ^{56}Ni yields must be $\lesssim 0.5 M_{\odot}$ and $\sim 0.1 - 0.2 M_{\odot}$ which are significantly smaller than $1 M_{\odot}$ ⁶. The kinetic energy of SN 2006nx

⁵Pejcha & Thompson (2014) demonstrated that in most cases the absolute value of the progenitor binding energy E_{bin} must be less than the neutrino-driven wind energy E_{wind} (i.e., E_{exp}) and the total energy $E_{\text{tot}} (= E_{\text{exp}} + E_{\text{bin}})$ is approximately equal to the wind energy E_{wind} , see their Fig. 12.

⁶ Although the kinetic energy of SN 14475 has rather significant uncertainty, its upper limit is only ~ 1.7

($\approx 2.160^{+3.753}_{-0.501} \times 10^{52}$ erg, Taddia et al. 2015) has rather significant uncertainty, but its upper limit ($\approx 5.91 \times 10^{52}$ erg) is slightly larger than that of SN 1998bw ($\approx 5 \times 10^{52}$ erg). Hence, the ^{56}Ni yield of SN 2006nx must be $\sim 0.5 M_{\odot}$ and smaller than $1 M_{\odot}$.

We can constrain the ^{56}Ni masses of SN 2010ay, SN 2006nx, and SN 14475 using another method. Umeda & Nomoto (2008) calculated the mass of the synthesized ^{56}Ni in CCSNe with progenitor Zero-Age Main-Sequence masses $M_{\text{ZAMS}} \leq 100 M_{\odot}$ and found that the typical ^{56}Ni mass is at most 20% of the ejecta mass. According to our light-curve modeling, the ejecta mass of SN 2010ay, SN 2006nx, and SN 14475 to be $6.5 M_{\odot}$, $3.6 M_{\odot}$, and $2.1 M_{\odot}$, respectively, see Table 1. Combining these two results, $\lesssim 1.3$, 0.7 , and $0.4 M_{\odot}$ of ^{56}Ni can be synthesized in the explosions, respectively.⁷ If the masses of ^{56}Ni are ~ 2.0 , 2.0 , and $1.3 M_{\odot}$, the values of $M_{\text{Ni}}/M_{\text{ej}}$ are ~ 0.31 , 0.56 , and 0.62 (see Table 1) which (far) exceed the upper limit (~ 0.2) of the mass ratio given by Umeda & Nomoto (2008) for CCSNe.

These results indicate that the ^{56}Ni -decay model cannot account for the light curves of SN 2010ay, SN 2006nx, and SN 14475 and these three SNe are probably solely or partly powered by other energy sources.

3.3. The magnetar spin-down energy model

Encountered by the above difficulty, alternative energy-reservoir models must be seriously considered. According to their inferred ratio of M_{Ni} to M_{ej} , ~ 0.2 , Sanders et al. (2012) suggested that SN ejecta-circumstellar medium interaction could also contribute to the high peak luminosity of SN 2010ay as well, yet they did not perform further investigation for this possibility. Owing to the lack of narrow and/or intermediate-width emission lines indicative of interactions between the SN ejecta and hydrogen- and helium-deficient CSM, we argue that ejecta-CSM interactions could hardly provide a reasonable interpretation for the excess luminosities of SN 2010ay, SN 2006nx, and SN 14475. Hence we attribute the luminosity excess instead to energy injection by the nascent magnetars and employ the magnetar model to explain the data for these SNe Ic.

The parameters for the magnetar model are listed in Table 1 and the light curves repro-

$\times 10^{52}$ erg, significant smaller than that of that of SN 1998bw, so we can expect that its ^{56}Ni mass should be smaller than that of SN 1998bw.

⁷It should be emphasized that these values are very rough and give rather loose upper limits. Nevertheless, real values of the masses of ^{56}Ni are difficult to be larger than them and the range of $0.1 - 0.5 M_{\odot}$ is reasonable for these SNe.

duced by the sets of parameters are shown in Fig. 1 (Models A3 and A4 for SN 2010ay, B3 and B4 for SN 2006nx, C3 and C4 for SN 14475). It can be seen from Fig. 1 that the magnetar model can well fit the data. These results indicate that this model can be responsible for the light curves of SN 2010ay, SN 2006nx, and SN 14475, i.e., SN 2010ay, SN 2006nx, and SN 14475 are probably powered by nascent millisecond (or ~ 10 ms) magnetars.

3.4. The hybrid (^{56}Ni + magnetar) model

When the ejecta masses of CCSNe are not very large, e.g., $\lesssim 2 M_{\odot}$, the ^{56}Ni synthesized are generally $\lesssim 0.1 M_{\odot}$, which contribute a minor fraction of the luminosity of luminous SNe and can be neglected in the fit. Inserra et al. (2013) demonstrated that the magnetar models without ^{56}Ni and with $\sim 0.1 M_{\odot}$ of ^{56}Ni are similar and therefore neglected the contribution from ^{56}Ni for their six SLSNe Ic.

However, SN 2010ay, SN 2006nx, and SN 14475 are not SLSNe and their ejected ^{56}Ni might have a mass of $\sim 0.1 - 0.5 M_{\odot}$, so the contribution from ^{56}Ni must be taken into account in our modeling.

Since the exact values of M_{Ni} of these three SNe are unknown when the contribution from magnetars is considered, we plot light curves corresponding to a variety of masses of ^{56}Ni . The typical values of M_{Ni} adopted here are 0.1, 0.2, 0.5 and $1.0 M_{\odot}$ ⁸. The parameters for the hybrid (^{56}Ni + magnetar) model are also listed in Table 1 and a family of light curves reproduced by these sets of parameters are shown in Fig. 1 (Models A5–A8 for SN 2010ay, B5–B8 for SN 2006nx, C5–C8 for SN 14475).

The ^{56}Ni mass with $\lesssim 0.5 M_{\odot}$, the energy released by the rapidly spinning magnetar is still the dominant energy source in powering the optical light curves of SN 2010ay, SN 2006nx, and SN 14475. When the ^{56}Ni mass is $\sim 1 M_{\odot}$, the energy released by ^{56}Ni is comparable with or exceed the energy released by the magnetar. If the ^{56}Ni masses are $\lesssim 1 M_{\odot}$ and the magnetar parameters are adjusted, the light curves reproduced by the hybrid model are all in good agreement with observations, indicating that $\lesssim 1 M_{\odot}$ of ^{56}Ni is admitted to be synthesized in their explosions.

On the other hand, there are rather significant discrepancies in the late-time ($\gtrsim 50$ days) light curves reproduced by different masses of ^{56}Ni . These discrepancies cannot be eliminated by adjusting the magnetar parameters since the decline rate of late-time light curves is

⁸Although we have demonstrated in Section 3.2 that the ^{56}Ni mass of these three SNe can hardly be larger than $0.5 M_{\odot}$, considering the possible uncertainties, we also adopt the value of $1.0 M_{\odot}$ in our modeling.

determined mainly by ^{56}Co decay rate and the value of κ_γ .

We cannot determine the precise masses of ^{56}Ni synthesized in the explosions of these SNe, because there is no precise late-time observation. Provided that there are some late-time data observed, it would be powerful enough to constrain the precise value of their ^{56}Ni mass.

To compare these models, we calculate the values of $\chi^2/\text{d.o.f}$ for all these theoretical light curves⁹, see Table 1. Since the ^{56}Ni -powered models are disfavored in explaining these three SNe, as discussed above, we do not discuss them here even if they give smaller $\chi^2/\text{d.o.f}$. Therefore, we only consider the magnetar-powered models and hybrid models. It can be seen from the last column in Table 1 that Models A4 (magnetar-powered model with hard emission leakage), B7 (magnetar and $0.5 M_\odot$ of ^{56}Ni), and C5 (magnetar and $0.1 M_\odot$ of ^{56}Ni) have the smallest $\chi^2/\text{d.o.f}$. Nevertheless, due to the absence of late-time data, we still cannot conclude that these models are most favorable ones.

3.5. An analysis for the origin of the kinetic energy

It is necessary to take into account the kinetic energy coming from the PdV work. The tapped rotational energy of a nascent magnetar ($E_{\text{NS}} \simeq 2 \times 10^{52} (P_0/1 \text{ ms})^{-2} \text{ erg}$) must be split into radiation energy (E_{rad}) and kinetic energy ($E_{\text{K,mag}}$). The former heat the ejecta, while the latter accelerate the ejecta. When $P_0 \sim 9 \text{ ms}$, $E_{\text{NS}} \simeq 3.0 \times 10^{50} \text{ erg}$. Even if all of the rotational energy of the putative magnetar is converted into kinetic energy of the ejecta¹⁰, $E_{\text{K,mag}} \approx E_{\text{NS}} \simeq 3.0 \times 10^{50} \text{ erg}$, it is still far less than the total kinetic energy ($E_{\text{K}} \gtrsim 5 \times 10^{51} \text{ erg}$) of SN 2010ay, SN 2006nx, as well SN 14475 and can therefore be completely neglected.

We now turn our attention to the neutrino-driven mechanism (Bethe & Wilson 1985). Hydrodynamic supernova simulations suggest that the neutrino-driven mechanism can produce SN energies $\lesssim 2 \times 10^{51} \text{ erg}$ (Ugliano et al. 2012), far less than the observed kinetic energy of $E_{\text{K}} \gtrsim 5 \times 10^{51} \text{ erg}$, indicating that there must be another mechanism accounting for the additional energy of $\gtrsim 3 \times 10^{51} \text{ erg}$. A popular scenario to explain energetic SNe

⁹Since Taddia et al. (2015) did not provide the observational errors of the data of SN 2006nx and SN 14475, we adopt a fiducial value for the error, $\sim 1.3 \times 10^{42} \text{ erg s}^{-1}$, which is the smallest error of the SN 2010ay data. the difference between the real values of errors and our adopted values should not change the $\chi^2/\text{d.o.f}$ significantly.

¹⁰The calculations performed by Woosley (2010) have shown that $E_{\text{K,mag}} \simeq 0.4 E_{\text{NS}}$ when $P_0 = 4.5 \text{ ms}$, $B = 1 \times 10^{14} \text{ G}$.

with kinetic energies $\gtrsim 10^{52}$ erg is the “collapsar” model involving a “BH-disk” system, in which the “BH-disk” system generates bipolar jet/outflow while the “disk wind” ensures that the progenitor star explodes and synthesizes enough amount of ^{56}Ni . However, our fittings have demonstrated that the newly formed magnetar did not collapse to a black hole at least several days after the explosion. Hence, the huge kinetic energy might stem from some magnetohydrodynamic processes (e.g., magnetic buoyancy, magnetic pressure, hoop stresses, etc) related to the proto-NS themselves (Wheeler et al. 2000) after which the magnetars inject their rotational energy to heat the ejecta and generate the light curves.

4. Discussion and Conclusions

Most type Ic CCSNe produce ^{56}Ni which release energy to the ejecta via cascade decay and central NSs which convert a portion of their rotational energy into heating energy of the ejecta via the magnetic dipole radiation. For almost all normal CCSNe, $\sim 0.1\text{--}0.7 M_{\odot}$ of ^{56}Ni are adequate to power the peak and post-peak decline of observational light curves and the contribution of NSs can be neglected¹¹. In contrast, for SLSNe Ic which are lack of evidence of interaction and cannot be explained by ^{56}Ni solely, millisecond NSs (magnetars) can supply almost all input power and the contribution of ^{56}Ni can be neglected.

For luminous SNe Ic with $-19.5 \gtrsim M_{\text{peak}} \gtrsim -21$ mag in any band, however, both contributions from ^{56}Ni and NSs cannot be neglected without detailed modeling since the ^{56}Ni permitted by completely explosive burning are usually inadequate to power the high peak luminosities while the production of $\sim 0.1\text{--}\sim 0.5 M_{\odot}$ of ^{56}Ni is reasonable and may contribute a significant portion of the total luminosity. Therefore, these “gap-filler” events which bridge normal SNe and SLSNe must be explained by a unified model which contain contributions from ^{56}Ni and NSs.

To illustrate the necessity of constructing the unified model, we select and apply this model to three luminous SNe Ic-BL, SN 2010ay, SN 2006nx, and SN 14475. We tested the possibility that the luminosity evolutions of SN 2010ay, SN 2006nx, and SN 14475 are solely governed by radioactive ^{56}Ni cascade decay using the semi-analytical method and demonstrated that too large amounts, roughly 2.0, 2.0, and 1.3 M_{\odot} of ^{56}Ni , are needed to power their peak luminosities, respectively. These results disfavor the ^{56}Ni model in

¹¹If the explosion leaves a BH or nothing (corresponding to the so-called “pair instability SNe” (Heger & Woosley 2002) rather than CCSNe), then no NS contributes luminosity to the SN and the SN is solely powered by ^{56}Ni ; if the explosion produces a transitional NS lasting about several hours or days the contribution of the NS to the light curve of the SN can also be neglected.

explaining the light curves of SN 2010ay, SN 2006nx, and SN 14475, since the ratios of M_{Ni} to M_{ej} are 0.31, 0.56, and 0.62, respectively, significantly exceeding the upper limit (~ 0.2) calculated for CCSNe (Umeda & Nomoto 2008).

Then we alternatively invoke the magnetar model to reproduce the light curves of SN 2010ay, SN 2006nx, and SN 14475 and show that the light curves reproduced can be well consistent with the observations, suggesting that SN 2010ay, SN 2006nx, and SN 14475 are probably powered by spin-down energy injection from newly born millisecond magnetars. It seems that the magnetar model can account for the light curves of these SNe and ^{56}Ni is not necessary to be introduced. However, a moderate amount of ^{56}Ni , $\sim 0.1 - 0.5 M_{\odot}$, can be expected in completely explosive burning of silicon shell and could give rather energy to those not very luminous SNe. So ^{56}Ni cannot be neglected when the SNe are not very luminous. Thus we use the hybrid model to fit these three SNe.

We set $M_{\text{Ni}} = 0.1, 0.2, 0.5$ and $1.0 M_{\odot}$ and find that $\lesssim 0.2 M_{\odot}$ of ^{56}Ni can not significantly influence the theoretical light curves while $\gtrsim 0.5 M_{\odot}$ of ^{56}Ni can effectively alters the shapes of the light curves, leading us to adjust the magnetar parameters to fit the observations. Therefore, all these models (^{56}Ni , magnetar, and hybrid), with different amount of ^{56}Ni (from 0 to 2 or $1.3 M_{\odot}$), fit the light curves equally well and can be unified into a unified model. Among these models, the ^{56}Ni model needs huge, unrealistic amounts of ^{56}Ni , resulting in over-high ratios of M_{Ni} to M_{ej} . In contrast, the magnetar model needs no ^{56}Ni and conflict with the basic theory of nuclear synthesis. The hybrid model is reasonable in explaining these luminous SNe.

These facts suggest that these three luminous SNe Ic are all powered by both ^{56}Ni and magnetars, indicating that the magnetars contribute a large fraction of but not all power in driving their light curves. So we can conclude that, when M_{peak} (in any band) is $\lesssim -21$ mag, the contribution of ^{56}Ni can be neglected in light-curve modeling; when $-21 \lesssim M_{\text{peak}} \lesssim -19.5$ mag, the contribution from the magnetar cannot be omitted in modeling while the contribution from ^{56}Ni must be considered seriously; but when $M_{\text{peak}} \gtrsim -19.5$ mag, the contribution of the magnetar can generally be neglected (but see Maeda et al. 2007).

It should be pointed out that the “fiducial cutoffs” -19.5 mag and -21 mag that divide the normal SNe, luminous SNe and SLSNe are artificially given and do not have unambiguous physical meanings. Although no consistent picture of these SNe Ic with rather different peak luminosities has emerged so far, it seems that they have similar physical nature and similar power sources, e.g., ^{56}Ni and newly born NSs (magnetars), while the former result in a relative narrow range of peak-luminosities owing to the existence of the upper limit of ^{56}Ni yields and thus the peak luminosities, the latter might produce a wide range of peak-luminosities since the period of newly born NSs can vary from several milliseconds to several seconds,

and magnetic field strength of them can be up to 10^{15} G. These two power sources could result in a continuous sequence of peak-luminosities, covering normal, luminous, and very luminous SNe Ic and unifying most of them into a whole category in which normal SNe are powered by slow-spinning NSs and ^{56}Ni , while luminous SNe and SLSNe are mainly powered by fast-spinning (millisecond) magnetar and ^{56}Ni . The similarity between late-time spectra of SLSNe Ic and spectra of normal SNe Ic-BL (Pastorello et al. 2010; Gal-Yam 2012; Inserra et al. 2013) also supports this unified picture.

Furthermore, we suggest that many SNe Ic with $M_{\text{peak}} \lesssim -19.5$ mag might be partly powered by a nascent magnetar, i.e., the very young SN remnants of the explosions may harbor magnetars. The discrepancy in brightness between luminous SNe Ic and SLSNe Ic stem mainly from the initial spin periods of the magnetars, the former have $P_0 \sim 7 - 15$ ms, while the latter have $P_0 \sim 1 - 6$ ms (Inserra et al. 2013; Nicholl et al. 2014). For luminous SNe Ic, power from magnetars with $P_0 \sim 10$ ms can become comparable to or exceed that from ^{56}Ni , and vice versa; for SLSNe Ic, millisecond magnetars usually overwhelm ^{56}Ni in powering them.

For the sake of completeness, both these two power sources must be taken into account in light-curve modeling. Nevertheless, we still emphasize that this unified scenario is especially important for the gap-filler SNe Ic since they, as aforementioned, are hardly powered solely by ^{56}Ni but ^{56}Ni can contribute a non-negligible portion of the luminosity and must be considered in modeling. Modeling for these luminous SNe can also help us to understand how normal SNe Ic relate to SLSNe Ic. Besides, even if a SN or superluminous SN that can be solely explained by the magnetar model, Fe line in its spectrum, if observed, must be explained by introducing a moderate amount of ^{56}Ni , because the magnetar model cannot explain Fe line (Kasen & Bildsten 2010). This is another advantage of the unified model. In the recent excellent review for SLSNe, Gal-Yam (2012) already noticed these “gap-filler” SNe and reckoned that they are likely to be intermediate events between radioactivity-powered SNe/SLSNe Ic and the SLSNe Ic powered by some other processes. Our analysis has confirmed this conjecture and furthermore demonstrated that these “intermediate events” are likely to have the same power sources and the difference between them and their lower-luminosity and higher-luminosity cousins are mainly due to the physical properties of the nascent neutron stars embedded in their debris.

While this unified energy-reservoir model seems reasonable for SN 2010ay, SN 2006nx, and SN 14475, the precise value of ^{56}Ni yields cannot be determined, indicating that the traditional method that suppose all power given by ^{56}Ni cascade decay is not always reliable in inferring the ^{56}Ni yields of CCSNe, especially for those luminous and very luminous ones. To discriminate these models and roughly determine the ^{56}Ni mass as well as the parameters

of the putative NSs, late-time ($\gtrsim 100 - 200$ d) data are required. Unfortunately, these three SNe are all lacking late-time observations, especially for SN 14475 whose luminosity measurements in the period between 25 and 35 days after the peak are rather uncertain.

Spectral analysis would be of outstanding importance in determining the precise values of ^{56}Ni and M_{ej} as well as the parameters of the NS parameters. In practice, detection and analysis of nebular emission from ^{56}Fe resulted from the ^{56}Ni cascade decay and other heavy elements are necessary for precise measurement of ^{56}Ni yields. The ejecta mass M_{ej} can significantly influence the rise time, shape, and peak luminosity as well as the ratio of M_{Ni} to M_{ej} of a SN, so it is also a very important quantity in modeling. Due to the uncertainty of optical opacity κ , M_{ej} cannot be precisely determined using solely the light-curve modeling (see Fig. 2). To get more precise value of the ejecta mass or at least a rigorous upper/lower limit, as performed by Gal-Yam et al. (2009) for SN 2007bi, nebular modeling are required.

The above procedures need very precise observations and spectral analysis lasting several hundred days after the detection of the first light. Unfortunately, no late-time photometric data and spectra have been observed for these three SNe, especially for SN 2006nx and SN 14475. We cannot get enough information to determine the precise masses of ^{56}Ni and the real values of magnetar parameters. Hence, we cannot distinguish among these model parameters and therefore to have a more precise scenario. We can expect that future high cadence multi-epoch UV–optical–NIR observations of the luminous SNe can pose stringent constraints on the parameters of the nascent NSs and ^{56}Ni yields.

We thank an anonymous referee for helpful comments and suggestions that have allowed us to improve this manuscript. We thank Xiangyu Wang, Yongfeng Huang, Xiaofeng Wang, Yongbo Yu, Jinjun Geng, Liangduan Liu and Junjie Wei for helpful discussion and comments. This work is supported by the National Basic Research Program (“973” Program) of China (grant Nos. 2014CB845800 and 2013CB834900) and the National Natural Science Foundation of China (grant Nos. 11033002 and 11322328). X.F.W was also partially supported by the One-Hundred-Talent Program, the Youth Innovation Promotion Association, and the Strategic Priority Research Program “The Emergence of Cosmological Structures” (grant No. XDB09000000) of the Chinese Academy of Sciences, and the Natural Science Foundation of Jiangsu Province (No. BK2012890).

REFERENCES

Arnett, W. D. 1979, ApJL, 230, L37

- Arnett, W. D. 1982, *ApJ*, 253, 785
- Ben-Ami, S., Gal-Yam, A., Mazzali, P. A., et al. 2014, *ApJ*, 785, 37
- Bethe, H. A., & Wilson, J. R. 1985, *ApJ*, 295, 14
- Bucciantini, N., Quataert, E., Arons, J., Metzger, B. D., & Thompson, T. A. 2008, *MNRAS*, 383, L25
- Cano, Z., de Ugarte Postigo, A., Pozanenko, A., et al. 2014, *A&A*, 568, 19
- Cappellaro, E., Mazzali, P. A., Benetti, S., et al. 1997, *A&A*, 328, 203
- Candia, P., Krisciunas, K., Suntzeff, N. B., et al. 2003, *PASP*, 115, 277
- Chatzopoulos, E., Wheeler, J. C., & Vinko, J. 2009, *ApJ*, 704, 1251
- Chatzopoulos, E., Wheeler, J. C., & Vinko, J. 2012, *ApJ*, 746, 121
- Chatzopoulos, E., Wheeler, J. C., Vinko, J., Horvath, Z. L., & Nagy, A. 2013, *ApJ*, 773, 76
- Chevalier, R. A. 1982, *ApJ*, 258, 790
- Chevalier, R. A., & Fransson, C. 1994, *ApJ*, 420, 268
- Chevalier, R. A., & Irwin, C. M. 2011, *ApJL*, 729, L6
- Chugai, N. N. 1994, *MNRAS*, 326, 1448
- Clocchiatti, A., & Wheeler, J. C. 1997, *ApJ*, 491, 375
- Contardo, G., Leibundgut, B., & Vacca, W. D. 2000, *A&A*, 359, 876
- Colgate, S. A., & McKee, C. 1969, *ApJ*, 157, 623
- Colgate, S. A., Petschek, A. G., & Kriese, J. T. 1980, *ApJL*, 237, L81
- Dai, Z. G., & Lu, T. 1998a, *A&A*, 333, L87
- Dai, Z. G., & Lu, T. 1998b, *PhRvL*, 81, 4301
- Dai, Z. G. 2004, *ApJ*, 606, 1000
- Dai, Z. G., & Liu, R. Y. 2012, *ApJ*, 759, 58
- Drake, A. J., Djorgovski, S. G., Mahabal, A., et al. 2009, *ApJ*, 696, 870

- Drout, M. R., Soderberg, A. M., Gal-Yam, A., et al. 2011, *ApJ*, 741, 97
- Drout, M. R. , Soderberg, A. M., Mazzali P. A., et al. 2013, *ApJ*, 774, 58
- Falk, S. W., & Arnett, W. D. 1977, *ApJS*, 33, 515
- Filippenko, A. V. 1997, *ARA&A*, 35, 309
- Gal-Yam, A., Mazzali, P., Ofek, E. O., et al. 2009, *Natur*, 462, 624
- Gal-Yam, A. 2012, *Science*, 337, 927
- Ginzburg, S., & Balberg, S. 2012, *ApJ*, 757, 178
- Hamuy, M. 2003, *ApJ*, 582, 905
- Heger, A., & Woosley, S. E. 2002, *ApJ*, 567, 532
- Hjorth, J., & Bloom, J. S., 2012, in Chapter 9 in *Gamma-Ray Bursts*, ed. C. Kouveliotou, R. A. M. J. Wijers, & S. Woosley (Cambridge Astrophysics Series, Vol. 51; Cambridge: Cambridge Univ. Press), 169
- Howell, D. A., Kasen, D., Lidman, C., et al. 2013, *ApJ*, 779, 98
- Inserra, C., Smartt, S. J., Jerkstrand, A., et al. 2013, *ApJ*, 770, 128
- Iwamoto, K., Mazzali, P. A., Nomoto, K., et al. 1998, *Natur*, 395, 672
- Janka, H.-T., Langanke, K., Marek, A., Martinez-Pinedo, G., & Müller, B. 2007, *Physics Reports*, 442, 1-6, 38
- Kasen, D., & Woosley, S. E. 2009, *ApJ*, 703, 2205
- Kasen, D., & Bildsten, L. 2010, *ApJ*, 717, 245
- Klein, R. I., & Chevalier, R. A. 1978, *ApJL*, 223, L109
- Kotera, K., Phinney, E. S., & Olinto, A. V. 2013, *MNRAS*, 432, 3228
- Lundqvist, P., Kozma, C., Sollerman, J., & Fransson, C. 2001, *A&A*, 374, 629
- Lyman, J. D., Bersier, D., James, P. A., Mazzali, P. A., Eldridge, J., Fraser, M., & Pian, E. 2014, *arXiv:1406.3667*
- MacFadyen, A. I., & Woosley, S. E. 1999, *ApJ*, 524, 262

- Maeda, K., Mazzali, P. A., Deng, J., Nomoto, K., Yoshii, Y., Tomita, H., & Kobayashi, Y. 2003, *ApJ*, 593, 931
- Maeda, K., Tanaka, M., Nomoto, K., Tominaga, N., Kawabata, K., Mazzali, P. A., Umeda, H., Suzuki, T., & Hattori, T. 2007, *ApJ*, 666, 1069
- Mazzali, P. A., Iwamoto, K., & Nomoto, K. 2000, *ApJ*, 545, 407
- Mazzali, P. A., Deng, J., Pian, E., et al. 2006, *ApJ*, 645, 1323
- McCrum, M., Smartt, S. J., Kotak, R., et al. 2014, *MNRAS*, 437, 656
- Metzger, B. D., Thompson, T. A., & Quataert, E. 2007, *ApJ*, 659, 561
- Metzger, B. D., Giannios, D., Thompson, T. A., Bucciantini, N., & Quataert, E. 2011, *MNRAS*, 413, 2031
- Moriya, T. J., Blinnikov, S. I., Tominaga, N., Yoshida, N., Tanaka, M., Maeda, K., & Nomoto, K. 2013, *MNRAS*, 428, 1020
- Nakamura, T., Mazzali, P. A., Nomoto, K., & Iwamoto, K. 2001, *ApJ*, 550, 991
- Nicholl, M., Smartt, S. J., Jerkstrand, A., et al. 2013, *Natur*, 502, 346
- Nicholl, M., Jerkstrand, A., Inserra, C., et al. 2014, *MNRAS*, 444, 2096
- Nugent, P. E., Sullivan, M., Cenko, S. B., et al. 2011, *Natur*, 480, 344
- Ofek, E. O., Sullivan, M., Cenko, S. B., et al. 2013, *Natur*, 494, 65
- Ostriker, J. P., & Gunn, J. E. 1971, *ApJL*, 164, L95
- Pastorello, A., Smartt, S. J., Botticella, M. T., et al. 2010, *ApJL*, 724, L16
- Pejcha, O., & Thompson, T. A. 2014, accepted to *ApJ*, arXiv:1409.0540
- Popov, D. V. 1993, *ApJ*, 414, 712
- Quimby, R. M., Kulkarni, S. R., Kasliwal, M. M., et al. 2011, *Natur*, 474, 487 and *Gamma-Ray Bursts*, ed. P. W.A. Roming, N. Kawai, & E. Pian (Cambridge: Cambridge Univ. Press), 22
- Sanders, N. E., Soderberg, A. M., Valenti, S., et al. 2012, *ApJ*, 756, 184
- Soderberg, A. M., Kulkarni, S. R., Fox, D. B., et al. 2005, *ApJ*, 627, 877

- Sollerman, J., Holland, S. T., Challis, P., et al. 2002, *A&A*, 386, 944
- Smith, N., & McCray, R. 2007, *ApJL*, 671, L17
- Stritzinger, M., & Leibundgut, B. 2005, *A&A*, 431, 423
- Strolger, L. G., Smith, R. C., Suntzeff, N. B., et al. 2002, *AJ*, 124, 2905
- Sutherland, P. G., & Wheeler, J. C., 1984, *ApJ*, 280, 282
- Taddia, F., Sollerman, J., Leloudas, G., Stritzinger, M. D., Valenti, S., Galbany, L., Kessler, R., Schneider, D. P., & Wheeler, J. C. 2015, *A&A*, 574, A60
- Uglikano, M., Janka, H.-T., Marek, A., & Arcones, A. 2012, *ApJ*, 757, 69
- Umeda, H., & Nomoto, K. 2008, *ApJ*, 673, 1014
- Usov, V V. 1992, *Natur*, 357, 472
- Valenti, S., Benetti, S., Cappellaro, E., et al. 2008, *MNRAS*, 383, 1485
- Valenti, S., Fraser, M., Benetti, S., et al. 2011, *MNRAS*, 416, 3138
- Vreeswijk, P. M., Savaglio, S, Gal-Yam, A., et al. 2014, *ApJ*, 797, 24
- Walker, E. S., Mazzali, P. A., Pian, E., et al. 2014, *MNRAS*, 442, 2768
- Wang, S. Q., Wang, L. J., Dai, Z. G., & Wu, X. F. 2015, *ApJ*, 799, 107
- Wheeler, J. C., Yi, I., Höflich, P., & Wang, L. 2000, *ApJ*, 537, 810
- Wheeler, J. C., Johnson, V., & Clocchiatti, A. 2014, *arXiv:1411.5975*
- Woosley, S. E. 1993, *ApJ*, 405, 273
- Woosley, S. E. 2010, *ApJL*, 719, L204
- Woosley, S. E., Heger, A., & Weaver, T. A. 2002, *Reviews of Modern Physics*, 74, 4, 1015
- Woosley, S. E., & Bloom, J. S. 2006, *ARA&A*, 44, 507
- Yuan, F., Quimby, R. M., Wheeler, J. C., et al. 2010, *ApJ*, 715, 1338
- Zhang, B., & Mészáros, P. 2001, *ApJL*, 552, L35
- Zhang, T. M., Wang, X. F., Wu, C., et al. 2012, *AJ*, 144, 131

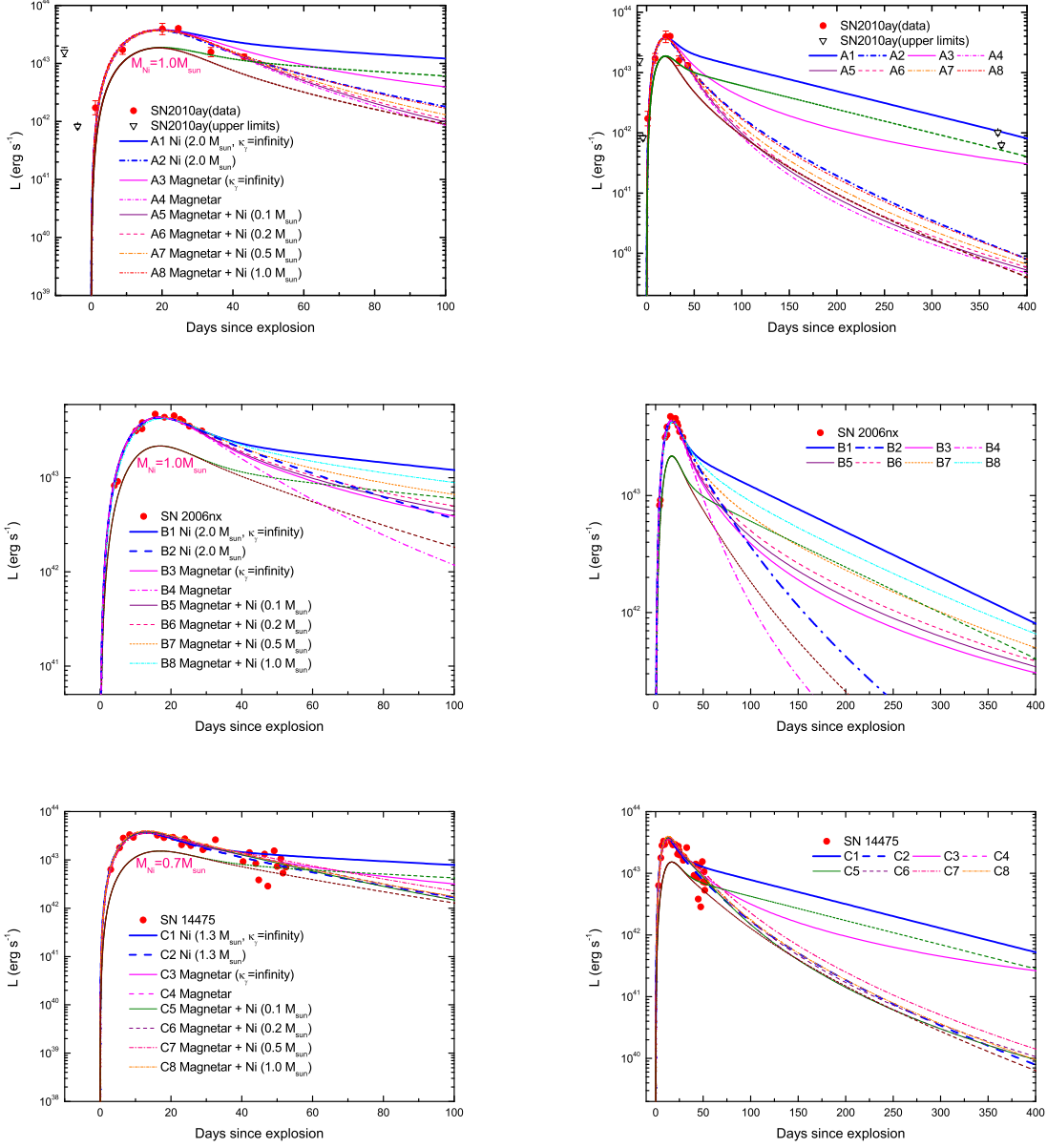
Table 1: Parameters for unified (^{56}Ni -decay, magnetar spin-down, and hybrid (^{56}Ni + magnetar)) modeling

	M_{ej} (M_{\odot})	B (10^{14} G)	P (ms)	v (c)	κ ($\text{cm}^2 \text{ g}^{-1}$)	κ_{γ} ($\text{cm}^2 \text{ g}^{-1}$)	M_{Ni} (M_{\odot})	$M_{\text{Ni}}/M_{\text{ej}}$	$\chi^2/\text{d.o.f}$
SN 2010ay									
Model A1 ^a	6.5	0	∞	0.064	0.07	∞	2.0	0.308	5.41
Model A2 ^a	6.5	0	∞	0.064	0.07	0.014	2.0	0.308	1.05
Model A3 ^b	6.5	4.5	8.8	0.064	0.07	∞	0	0	2.36
Model A4 ^b	6.5	4.5	8.8	0.064	0.07	0.021	0	0	1.34
Model A5 ^c	6.5	4.5	9.0	0.064	0.07	0.021	0.1	0.015	2.00
Model A6 ^c	6.5	4.5	9.3	0.064	0.07	0.021	0.2	0.031	2.05
Model A7 ^c	6.5	5.2	10.3	0.064	0.07	0.021	0.5	0.077	2.11
Model A8 ^c	6.5	7.2	12.5	0.064	0.07	0.021	1.0	0.154	2.12
SN 2006nx									
Model B1 ^a	3.6	0	∞	0.051	0.07	∞	2.0	0.556	1.24
Model B2 ^a	3.6	0	∞	0.051	0.07	0.037	2.0	0.556	1.22
Model B3 ^b	3.6	4.5	8.8	0.051	0.07	∞	0	0	1.58
Model B4 ^b	3.6	4.5	8.8	0.051	0.07	0.037	0	0	1.56
Model B5 ^c	3.6	4.5	9.0	0.051	0.07	∞	0.1	0.028	1.60
Model B6 ^c	3.6	4.5	9.2	0.051	0.07	∞	0.2	0.056	1.44
Model B7 ^c	3.6	4.5	9.8	0.051	0.07	∞	0.5	0.139	1.11
Model B8 ^c	3.6	4.8	11.9	0.051	0.07	∞	1.0	0.278	1.60
SN 14475									
Model C1 ^a	2.1	0	∞	0.062	0.07	∞	1.3	0.619	4.10
Model C2 ^a	2.1	0	∞	0.062	0.07	0.063	1.3	0.619	2.78
Model C3 ^b	2.1	4.8	10.4	0.062	0.07	∞	0	0	3.03
Model C4 ^b	2.1	4.8	10.4	0.062	0.07	0.133	0	0	3.30
Model C5 ^c	2.1	4.8	10.7	0.062	0.07	0.133	0.1	0.048	2.97
Model C6 ^c	2.1	4.8	10.9	0.062	0.07	0.133	0.2	0.095	3.53
Model C7 ^c	2.1	4.8	12.6	0.062	0.07	0.133	0.5	0.238	3.54
Model C8 ^c	2.1	4.8	15.2	0.062	0.07	0.063	1.0	0.476	4.03

^a The ^{56}Ni -decay model.

^b The magnetar model.

^c The hybrid (^{56}Ni + magnetar) model.



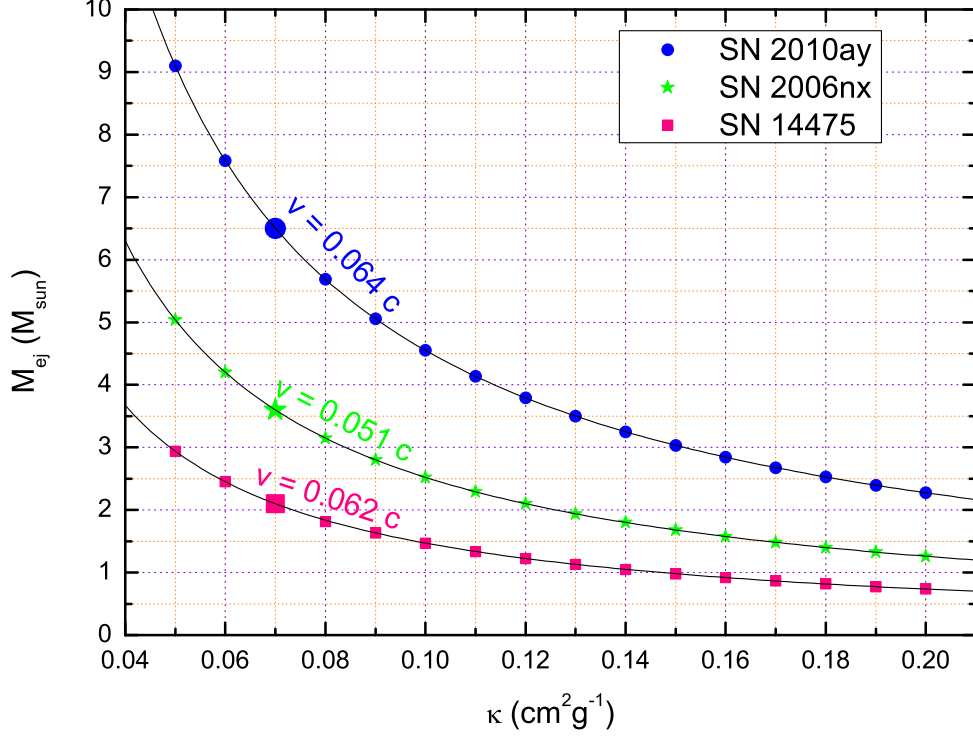


Fig. 2.— The values of κ vs. the values of M_{ej} for SN 2010ay, SN 2006nx, and SN 14475. The values of κ vary from $0.05 \text{ cm}^2 \text{g}^{-1}$ to $0.20 \text{ cm}^2 \text{g}^{-1}$, resulting in rather different values of M_{ej} required. Big Circle, Star, and Square correspond to SN 2010ay, SN 2006nx, and SN 14475 with $\kappa = 0.07 \text{ cm}^2 \text{g}^{-1}$, respectively.